2021 43rd Annual International Conference of the
IEEE Engineering in Medicine & Biology Society (EMBC)
Oct 31 - Nov 4, 2021. Virtual Conference

Design and 3D Printing of Four Multimaterial Mechanical Metamaterial Using PolyJet Technology and Digital Materials for Impact Injury Prevention

Cesar S. Carrillo and Midori Sanchez

Abstract— **Impact injuries are very common daily problems in sports. Over the last years there has been advances in the prevention of impact injuries with the creation of new energy-absorbing materials, but the field is still novel. Mechanical metamaterials are three-dimensional materials whose mechanical properties are strongly related to its structure and not only to the material of which they are made. The materials showed in this work are composed of various unit cells with a specific geometry. Because of the unit cells' complex architecture, 3D printers are more convenient to manufacture them. Thus, PolyJet is a perfect technology for metamaterials because it allows printing complex structures with high resolution and mixing the raw materials in order to obtain different properties such as flexibility and shock absorption.**

In this work, we aim to analyze the printing parameters of the Octet-Truss Lattice, Kelvin Foam, Convex-Concave Foam and Truss-Lattice auxetic unit cells (UC). In addition, the structures are composites of VeroPlus and Agilus. Finally, we 3D-printed all the metamaterials designed using the PolyJet printer Objet 500 Connex 3 to analyze the feasibility of manufacturing with suitable parameters. The results showed that the support material in the printing of the UC made of Truss-Lattice and Kelvin Foam could be removed more easily than in the Octet-Truss Lattice and Convex-Concave Foam. This happened because of the free space between the beams in the UC.

I. Introduction

Impact injuries (IJ) occur daily in any accident involving moving vehicles. The extent of injury depends upon the velocity, distance travelled, duration of impact, direction of impact, and absorption of stresses by the body or objects struck [1]. Moreover, they occur in contact sports such as soccer, rugby, running or car racing. These impacts in sports can cause severe and fatal head, spinal and thoracic injuries. For these reasons, sports have developed methods and equipment to prevent IJ, such as rule modifications, helmets, insoles, padded clothing and training to avoid traumas [2]. There are advances in injury prevention with new energy absorbing materials [3]. Nowadays, the most used are foams or silicones within fabrics to protect them, but these materials tend to wear out, permanently deform or break easily. On the other hand, a new branch of research is being explored with more resistant and shock-absorbing materials, with optimization of weight and with structures that are comfortable for users, as they are more ventilated and prevent sweating. These materials are known as metamaterials (MM), which are three-dimensional materials to whit an architecture that confers them their special properties that cannot be found naturally. In that sense, they are materials created and designed by humans from micro to macro scales to provide improved properties and functionalities. This special structure is composed of various unit cells (UC) with a well-defined geometry. The MM are differentiated by their applications: mechanical, thermal, optical, electrical, acoustic, and transport [4] [5]. In the past few years, the concept of Mechanical Metamaterial (MMM) has gained the attention in the scientific community due to exceptional mechanical properties [6]. Their most studied property is the negative Poisson's ratio [7] [8] [9]. In this way, the MMM can be divided into two groups: the MMM with negative Poisson's ratio, better known as auxetic metamaterials, and the ones with positive Poisson's ratio [6] (see Fig. 1). Therefore, in this work, the design and manufacturing process of different structural designs of metamaterials with improved mechanical properties for energy absorption will be shown.

The architecture and design confer the MMM their properties, which is why several kinds of structures of UC exist, like Octet-Truss Lattice (OTL) [10], Kelvin Foam (KF) [10], Convex-Concave Foams (CCF) [11], and Truss lattice (TL) [12]. Each one of these structures gives MMM different mechanical properties. The geometries of the MM are complex and require a special technology of manufacturing. Over the last years, new 3D printing methods have been developed which use different technologies. One of these technologies is the PolyJet which, according to Stratasys, is a powerful 3D printing technology based on the deposition of micrometric layers of photo polymeric resin producing smooth and accurate parts. With a micrometric layer resolution and an accuracy of 0.014 mm, it can produce thin walls and complex geometries using the widest range of materials available with any technology [13]. Due to these characteristics, it has been recently used to print MM [14] [15] [16]. Stratasys has developed special materials that can only be printed in PolyJet and have particular mechanical

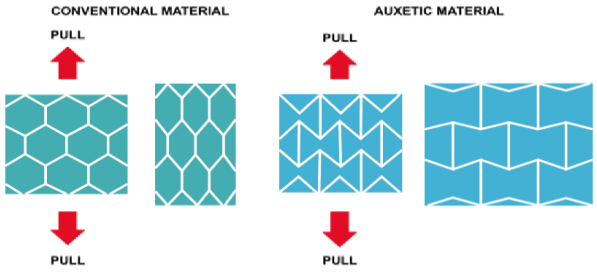

Fig. 1. On the left, we can see an example of conventional material and on the right we can see an example of an auxetic material. The deformation is the key characteristic

Cesar S. Carrillo (cesar.carrillo@pucp.edu.pe) is a university student of biomedical engineering in the universities of Pontificia Universidad Católica del Perú (PUCP) and Universidad Peruana Cayetano Heredia (UPCH).

Midori Sanchez (sanchez.ac@pucp.edu.pe) is a master of materials science and engineering, and a bachelor in science with mention on mechatronics engineering from the PUCP, currently is an investigator in the Digital Manufacturing Lab VEO 3D of the Engineering Department of the PUCP.

properties (see in Table I). In order to obtain a resistant auxetic structure, a rigid material is needed that provides mechanical resistance and is immersed or mixed with a flexible material, which is responsible for elasticity and resistance to impacts. With these characteristics, the one most studied is VeroPlus, which is a rigid material and comes in different colors [17]. Another relatively new material is the Agilus 30 that is a soft and flexible material, but it is capable of withstanding repeated flexing and bending. VeroPlus and Agilus are the most used in Polyjet, because of their printability and costs; therefore, they were chosen for the study of this project. Despite being the most widely used and found materials in the literature, there are not many studies about their applications. Thus, the properties and the capability of the PolyJet technology to print the MM needs further research.

This work aims to analyze the printing parameters of the MM made with structures of UC of OTL, KF, CCF and TL. The first step is the design of the UC of OTL, KF, CCF and TL. Secondly, we will create a structure that contains various UC for the printing of the MM. Lastly, the designs are going to be printed in the Objet500 Connex3 PolyJet 3D printer. In addition, we will use the materials Veroplus and Agilus 30 mixing them in the structure giving the MMM different mechanical properties.

TABLE I. MECHANICAL PROPERTIES OF VEROPLUS AND AGILUS 30

Mechanical properties	**Material**	
	VeroPlus	*Agilus 30*
Tensile Strength	58 MPa	2.1-2.6 MPa
Elongation at Break	10% - 25%	185 – 230%
Shore Hardness	85 D	30 – 40 Scale A

II. DESIGN OF METAMATERIALS

Developing good UC's structures is key to achieve good results. In this chapter, we will show how the four UC were created. For all the UC the software Autodesk Inventor 2021 was used, because of its versatile functions and capability to create complex structures. Below, the types of UC to create MM and the measures that were designed are shown.

A. Octet-Truss lattice.

OTL is a structure with open-cell intermediate face sheets between the layers of inclined beams, which is a more efficient foam than other ones with similar in density and material quantity. This made the MM made of OTL attractive to study [18]. In Fig. 2.A, we can see the OTL UC. In Fig. 2.B, we can see a MM made of OTL UC. For the design, the measures taken were L and R, being L the total length of the UC and R the radius of the beams, see it in Fig. 2. I.

B. Kelvin Foam.

In 1887, Lord Kelvin, created the "perfect foam" which cells are shaped like a truncated octahedron, with eight hexagonal faces and six square ones, in this way providing the faces a little curvature in order to better fit Plateau's rules [19]. In Fig. 2. C, we see the KF UC. In Fig. 2. D, we can see the MM made of KF UC. For the design, the measures taken were D, L and R, being L the distance of one side of the squares, D is the total length of the UC and R is the radius of the beams, we can see it in Fig. 2. J.

C. Convex-concave foams.

The CCF takes its inspiration from the conventional open foam, which consists of eight edges straight beams. The difference is that CCF shifts with a tunable curvature of the beams and gives the MM different properties [10]. In Fig. 2. E, we can see the CCF UC. In Fig. 2. F, we can see a MM made of CCF UC. For the design, the measures taken were L, T, and H, being L the edge total length of the UC, T is the thickness of the edge and H is the total height shift of the beams, as we can see in Fig. 2. K.

D. Truss-lattice.

The TL consists of 4 edges connecting one corner and is immediately opposite of an invisible cube. In Fig. 2. J, we can see the TL UC. In Fig. 2. H, we can see a MM made of TL. For the design, the measures taken were L and r, being L the total length of the UC and R is the radius of the beams, as we can see in Fig. 2. L.

In Table II we can see the measures taken for every UC. Finally, the structures that will be printed were created. All structure will consist on 16 UC making a layer of UC of 40

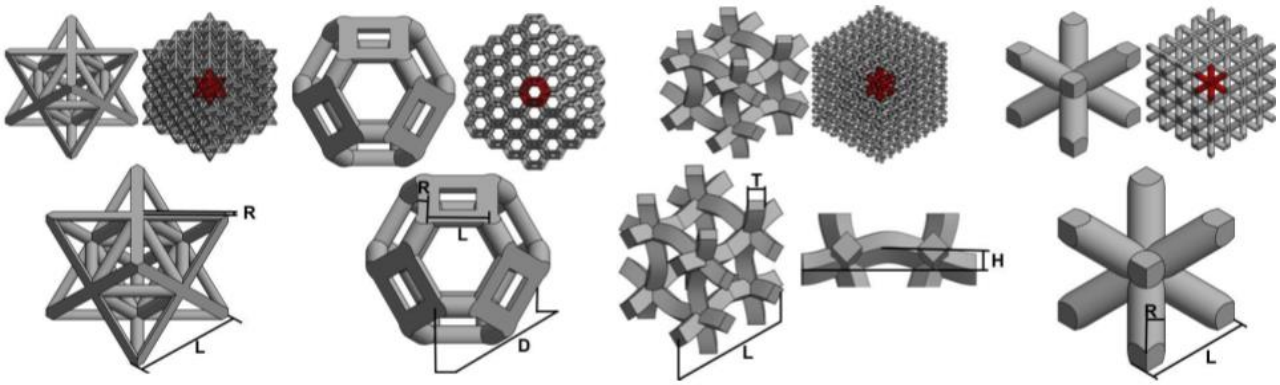

Fig. 2. We can see that A, B and I refer to the TL; C, D and J, to CCF; E, F and K, to OTL; G, H and L, to KF. In A we can see the unit cell of OTL, in B we can see the MM made of UC of OTL and in I we can see the unit cell of OTL with the parameters that were taken for its creation. In C we can see the unit cell of KF, in D we can see the MM made of UC of KF and in J we can see the unit cell of KF with the parameters that were taken for its creation. In E we can see the unit cell of CCF, in F we can see the MM made of UC of CCF and in K we can see the unit cell of KF with the parameters that were taken for its creation. In G we can see the unit cell of TL, in H we can see the MM made of UC of TL and in L we can see the unit cell of TL with the parameters that were taken for its creation.

mm x 40 mm x 10 mm (Length, Thickness, and Height). In addition, a top was created for the bottom of every structure with dimensions of 40 mm x 40 mm x 2 mm. In that way, the final dimensions of the structure were 40 mm x 40 mm x 12 mm. In addition, a MM made from TL of 40 mm x 40 mm x 40 mm was printed. This size was chosen based on future mechanical tests that will be performed. As they are composite materials, according to the standards ASTM D638, C364, C394 for tensile, compression and tear respectively, it must have a minimum thickness to accurately measure the new properties and not have uncertainties of some flaws.

TABLE II. VARIATIONS OF UC

Name	*L (mm)*		*R (mm)*
TL	10		0.5
Name	*D (mm)*	*L (mm)*	*R (mm)*
KF	10	2	0.5
Name	*L (mm)*	*T (mm)*	*H (mm)*
CCF	10	1	1
Modification	*L (mm)*		*R (mm)*
OTL	10		0.5

Since we are using two materials, we printed different configurations for the UCs, because it could change the mechanical properties. The first type of combinations is special for UC of CCF. The CCF's beams were grouped in two: the vertical ones and horizontal ones. The configuration consists of the horizontal beams made of one material and the rest with another material (HB), as can see in Fig. 3. A. The second configuration is special for UC of OTL. The OTL's beams are grouped in two: the beams in the perimeter and the center ones. The configurations consist of the beams located in the perimeter are printed on one material, and the rest of the beams with another material (PC), we can see in Fig. 3. B. The last configuration is the Meta sandwich (MS), which consists of changing the material between layers of the MM, the first two layers made from one material and the next one of another material, it keeps repeating until the MM ends (see in Fig. 3. C). This configuration is going to be used in the MM. The TL and KF structures were printed on VeroBlackPlus (Rigid material). Also, the horizontal beams of the CCF HB structure were made of VeroBlackPlus and the rest of the beams with Agilus30 clear (Flexible material). On the other hand, the beams located in the perimeter of the OTL PC were printed on VeroBlackPlus and the beams located in the center with Agilus30 clear.

III. PRINTING PROCESS

Before printing, the structures need to go through a process that guarantees the quality and maintains the watertight [20] property of the STL file. The software

Fig. 3. We can see the different configurations used in this investigation, the red color represents Agilus 30 Clear and the gray color represents the VeroBlackPlus. In A we can see the configuration of CCF, CCF-HB. In B we can see configuration OTL-PC. In C we can see the MS configuration of the MM.

Autodesk Netfabb helps with this analysis and in some cases, it patch the model. Then, we proceed to print them in the PolyJet 3D printer Objet500 Connex3, the software used was GrabCad Print and as we mentioned, the tray materials were VeroBlackPlus and Agilus30 clear. The print mode was set to digital materials in order to mix to different materials. The part has a resolution of 30 micrometers. The surface finish of the materials was matte and the layer thickness was 16 micrometers. Since the MM have complex architectures, the material for the support was SUP706B because this material could be removed with a solution and in an easier way than other support material. The post processing consisted of the removal of the support, so MM were immersed in solution of 2% of caustic soda in water for 2 hours, if the support didn't remove the water jet of the printer was used.

IV. RESULTS AND DISCUSSION

All structures were printed simultaneously and they took 18 hours to print. The first structure we can see is the TL (see in Fig. 4. A. and Fig. 4. B) and the second structure we can see is the one made of KF (see Fig. 4. C. and Fig. 4. D). All the support material was successfully removed, but the cleaning procedure broke beams located in the perimeter of the structure in both designs. This helps to infer that Agilus, which is a soft material, is required to resist impacts and a higher thickness should also be used. The third structure was the CCF HB (Fig. 4. E. and Fig. 4. F) and the fourth one OTL PC (Fig. 4. G. and Fig. 4.H). In both cases the support could not be removed totally; therefore, it was not possible to inspect the internal structure of the MM and we could not assure if any beam was broken or the functionality of the MM. For that reason the design had to be changed, in order to increase the space or separation of walls, at least 1.5mm. The last structure we see is the TL MM MS, where all the support was removed and no beams were broken (see Fig. 4. I).

The TL and KF structures had a bigger separation between the beams. That is why the support could be removed totally by the water jet. On the other hand, the water jet broke UC's beams located in the perimeter, the radius of the beams and the hard material (VeroBlackPlus). One

Fig. 4. In this figure we see the printing results. In A and B we can see the TL structure's printing. In C and D we can see the KF structure's printing. In E and F we can see the CCF-HB structure's printing. In G and H we can see the OTL.PC structure's printing. In I we can see the TL MM-MS's printing.

feasible reason for this is the small beams' radius. This must be increased in order to be capable to resist the pressure of the water jet. The new radius will be no less than 0.75 mm. In addition, the UCs broken in the perimeter could be improved by creating a thin wall that could reinforce their borders and then would remove cutting them. Furthermore, in the CCF HB and OTL PC, the support could not be removed. This can be explained by the complex architecture and the lack of free space. The complex architecture of the UC required more support material to be correctly printed and the number of beams decreased the free space between them. Then, when the water jet cleaned the structure, it could not reach all parts of the UC; therefore, the support was still in the center of the structure. This could be fixed by redesigning to add more space between the UC. The MM was perfectly printed in the PolyJet technology and the MS configuration gave the MM different mechanical and physical properties such as the weight and tensile strength. As the Table III shows for a block of 40x40x40mm the weight comparison is: Foam<MS<Silicone. This compares our design with the two materials more used in the applications of shock absorbers. Moreover, the tensile strength comparison is Foam<Silicone<MS. For that reason, the MS design is optimum to use IJ prevention, because low weight and high strength protectors could be manufactured using this configuration.

TABLE III. PROPERTIES OF COMPOSITE AND USUAL MATERIALS

Composite or Material	Property	
	Weight	*Tensile strength*
MS	40g	10 – 30 MPa
Foam	10g	1 – 6 MPa
Silicone	90g	2 – 15 MPa

V. CONCLUSIONS AND FUTURE WORK

The PolyJet 3D-printer and digital materials technology are capable of printing complex architectures to create MM. All dimensions of the MM must be carefully decided, in order to have enough space between beams to remove all of the support material. The optimum MM designed in this work is the MS. Also, it is known that MM have the capability to absorb impacts because of their auxetic design and the deformation in the three axes which helps to absorb the energy of an impact, making it useful to IJ prevention.

The next step for this project is to analyze the mechanical properties of each of the MM created, given that optimal design and slicing parameters were determined. Tensile, compression, shear, creep and relaxation tests will be performed. Additionally, the new metamaterials with the mixed properties of a rigid and flexible material will be characterized. Then, the results will serve to apply this new composite in biomedical and biomechanical applications, focusing in the field of IJ prevention using the MM.

ACKNOWLEDGMENT

In loving memory of C. C.'s father, who sadly passed away the day after receiving the acceptance letter. We know he would have been proud of his son's achievements.

REFERENCES.

[1] "Impact injury | trauma", Encyclopedia Britannica, 2021. [Online]. Available: https://www.britannica.com/science/impact-injury. [Accessed: 03- Mar- 2021].

[2] A. McIntosh, "Impact Injury in Sport", IUTAM Symposium on Impact Biomechanics: From Fundamental Insights to Applications, vol. 124, pp. 231-245, 2005. Available: 10.1007/1-4020-3796-1_24 [Accessed 3 Mar 2021].

[3] J. Patalak and J. Stitzel, "Evaluation of the effectiveness of toe board energy-absorbing material for foot, ankle, and lower leg injury reduction", Traffic Injury Prevention, vol. 19, no. 2, pp. 195-200, 2017. Available: 10.1080/15389588.2017.1354128 [Accessed 3 March 2021].

[4] S. C. Fischer, L. Hillen y C. Eberl, «Mechanical Metamaterials on the Way from Laboratory Scale to Industrial Applications: Challenges for Characterization and Scalability,» Materials, vol. 13, nº 16, p. 3605, 2020.

[5] C. P. De Jonge, H. M. A. Kolken y A. A. Zadpoor, «Non-Auxetic Mechanical Metamaterials,» Materials, vol. 12, nº 4, p. 635, 2019.

[6] A. A. Zadpoor, «Mechanical meta-materials,» Materials, vol. 3, nº 5, p. 365–462, 2016.

[7] S. Babaee, J. Shim, J. C. Weave, E. R. Chen, N. Patel y K. Bertoldi, «3D Soft Metamaterials with Negative Poisson's Ratio,» Advanced Materials, vol. 25, nº 36, p. 5044–5049, 2013.

[8] L. Ai y . X.-L. Gao, «Metamaterials with negative Poisson's ratio and non-positive thermal expansion,» Composite Structures, vol. 162, pp. 70-84, 2017.

[9] L. Ai y X.-L. Gao, «Three-dimensional metamaterials with a negative Poisson's ratio and a non-positive coefficient of thermal expansion,» International Journal of Mechanical Sciences, vol. 135, pp. 101-113, 2018.

[10] C. Yang, . M. Boorugu, A. Dopp, . J. Ren, R. Martin, D. Han, W. Choi y H. Lee, «4D Printing Reconfigurable, Deployable and Mechanically Tunable Metamaterials,» Materials Horizons, vol. 6, pp. 1244-1250, 2019.

[11] S. Cui, B. Gong, Q. Ding, Y. Sun, F. Ren, X. Liu, Q. Yan, H. Yang, X. Wang y B. Song, «Mechanical Metamaterials Foams with Tunable Negative Poisson's Ratio for Enhanced Energy Absorption and Damage Resistance,» Materials, vol. 11, nº 10, p. 1869, 2018.

[12] C. Xueyan, J. Qingxiang, J. Wei, H. Tan, J. Yu, P. Zhang, K. Muamer y V. Laude, «Light-weight shell-lattice metamaterials for mechanical shock absorption,» International Journal of Mechanical Sciences, vol. 169, p. 105288, 2019.

[13] «Stratasys,» [On line]. Available: https://www.stratasys.com/polyjet-technology. [Accessed: 21 March 2021].

[14] M. Bodaghi y W. H. Liao, «4D printed tunable mechanical metamaterials with shape memory operations,» Smart Materials and Structures, vol. 28, nº 4, 2019.

[15] M. Bodaghi, A. Damanpack y W. Liao, «Adaptive metamaterials by functionally graded 4D printing,» Materials and Design, vol. 135, pp. 26-36, 2017.

[16] R. Vdovin, T. Tomilina, V. Smelov y M. Laktionova, «Implementation of the additive PolyJet technology to the development and fabricating the samples of the acoustic metamaterials,» Procedia Engineering, vol. 176, pp. 595-599, 2017.

[17] Y. L. Tee, C. Peng, P. Pille, M. Leary y P. Tran, «PolyJet 3D Printing of Composite Materials: Experimental and Modelling Approach,» JOM, vol. 72, p. 1105–1117, 2020.

[18] L. Dong, V. Deshpande y H. Wadley, «Mechanical response of Ti–6Al–4V octet-truss lattice structures,» International Journal of Solids and Structures, Vols. %1 de %260-61, pp. 107-124, 2015.

[19] P. Ball, «NATURE,» 28 November 2011. [On line]. Available: https://www.nature.com/news/scientists-make-the-perfect-foam-1.9504#:~:text=The%20Weaire%2DPhelan%20foam%20is%20the%20perfect%20foam.&text=The%20Irish%20scientist%20Lord%20Kelvin,to%20better%20fit%20Plateau's%20rules.[Accessed:21March 2021].

[20] «Autodesk,» 02 January 2017. [On line].Available:https://knowledge.autodesk.com/support/moldflow-insight/learn-explore/caas/CloudHelp/cloudhelp/2017/ENU/MoldflowInsight/files/A%20watertight%20model%20is%20defined,holes%20or%20non%2Dmanifold%20ed. [Accessed: 28 March 2021].